

θ pinch in narrow-band semiconductors following transverse breakdown

S. M. Abdurakhmanov, V. V. Vladimirov, and V. N. Gorshkov

Physics Institute, Ukrainian Academy of Sciences

(Submitted 29 April 1983)

Zh. Eksp. Teor. Fiz. **85**, 2128–2134 (December 1983)

A theory of the θ pinch in semiconductors is developed for the first time ever. It describes the effect under transverse breakdown, when an electron-hole plasma is created and is pinched towards the sample axis by a magnetic field whose strength increases with time and by the transverse electric fields induced by the magnetic fields. The calculations are performed for narrow-band compounds (n -InSb and n -Bi $_{1-x}$ Sb $_x$), where the effect is most prominent. Linear, harmonic, and combined magnetic-field pulses are considered. Also determined are the conditions for optimal pinching of the plasma via nondiffusive penetration of a magnetic field into the plasma by a mechanism due to an ambipolar plasma flux of Hall-effect origin.

PACS numbers: 71.45.Gm, 71.35.+z

1. One of the contactless methods of obtaining a high-density nonequilibrium plasma in semiconductors is the θ pinch, when the plasma is pressed towards the sample axis by a longitudinal magnetic field that increases with time.¹ Since the carrier-momentum relaxation time in semiconductors is very short (10^{-11} – 10^{-12} sec), the inertia of the electrons and holes plays no role whatever in the θ -pinch dynamics, and the plasma is pinched as a result of ambipolar drift of the particles in the longitudinal magnetic field ($H \parallel z$) and by the azimuthal electric field it induces.

The θ pinch was investigated in greatest detail experimentally²⁻⁴ and theoretically^{5,6} in InSb and Ge, in the intrinsic-conductivity region (at room temperature), when the pulsed magnetic field and the electric fields induced by it play no decisive role in the plasma formation. In this case the electron and hole mobilities $b_{e,h}$ are relatively small and a noticeable pinching effect occurs only in strong magnetic fields, since this calls for the satisfaction⁵ of the condition $h^2 = b_e b_h H^2 / c^2 \gg 1$, where H is the magnetic-field amplitude; the magnetic-field pulse duration should be shorter here than the carrier lifetime. Hubner and Schneider have shown in their experiments⁴ that in n -InSb at low temperatures ($T_c = 140$ K), when the electron and hole mobilities are high, a θ pinch leads to a very strong increase of the plasma density, via transverse breakdown and subsequent pinching of the plasma. The plasma is then formed as a result of interband breakdown in the magnetic field crossed with the azimuthal electric field induced by it and with the radial electric Hall field (transverse breakdown⁷).

No theory was developed before for a θ pinch in the transverse-breakdown regime, when a pulsed magnetic field produces and pinches the plasma. In the present study we have performed the corresponding calculations for n -InSb ($T_c = 77$ K) and n -Bi $_{1-x}$ Sb $_x$ ($T_c = 4.2$ K), using the experimental dependences of the impact ionization^{8,9} and of the electron mobility^{10,11} on the electric field.

We note that performance of the corresponding experiments on n -Bi $_{1-x}$ Sb $_x$, where the band gap is small and the antimony content is varied, is of practical interest in connection with development of a source of submillimeter radiation (the recombination radiation is extracted through the end faces of the sample).

2. Using the equations of motion for the electrons and holes, the continuity equation, and Maxwell's equations, it is possible to obtain a system of two equations for the plasma density and for the magnetic field, as was done in Ref. 6. In the case of cylindrical geometry and a nondegenerate plasma this system takes the form

$$\frac{\partial N}{\partial T} + \frac{1}{\rho} \frac{\partial}{\partial \rho} (\rho \Gamma_0) = G(N+1) - RN(N+1), \quad (1)$$

$$\frac{\partial h}{\partial T} = \frac{\beta^2}{\rho} \frac{\partial}{\partial \rho} \left[\rho \frac{\gamma(E_\varphi, N)}{N+1} \frac{\partial h}{\partial \rho} \frac{\Psi(h, N)}{\Phi(h, N)} \right] + \frac{1}{\tau_D \rho} \frac{\partial}{\partial \rho} \left[\rho \frac{2N+1}{(N+1)^2} h \Phi^{-1}(h, N) \frac{\partial N}{\partial \rho} \right], \quad (2)$$

where $N = n/n_0$, n is the density of the electron-hole pairs, n_0 is that of the donors, $T = t/\tau$, and t is the time; in the case of a sinusoidal magnetic-field pulse ρ is equal to the period of the pulse, $\rho = r/R_0$, R_0 is the sample radius, Γ_0 is the radial ambipolar flux,

$$\Gamma_0 = - \left(\frac{1}{\tau_D} \frac{2N+1}{N+1} \frac{\partial N}{\partial \rho} + \beta^2 \frac{N}{N+1} h \frac{\partial h}{\partial \rho} \right) \Phi^{-1}(h, N),$$

$\tau_D = R_0^2 / \tau D_h$, D_h is the hole diffusion coefficient, $\gamma(E_\varphi, N) = \hat{b}_e / b_e$, \hat{b}_e a normalization constant ($\hat{b}_e = 10^8$ cgs esu for n -InSb and 7.5×10^8 for n -Bi $_{1-x}$ Sb $_x$), $b_e = b_{e0}(E_\varphi) / (1 + \alpha N)$, the $b_{e0}(E_\varphi)$ dependence was approximated to fit the experimental data,^{10,11} α is the parameter of the electron-hole scattering¹² (assumed equal to 10^{-2} , $\beta^2 = c^2 \tau / 4\pi n_0 \hat{b}_e R_0^2 = \tau / \tau_M$, where τ_M is the characteristic diffusion time of the magnetic field, $G = g\tau$, $g(E_\varphi, E_r)$ is the impact-ionization coefficient, $R = \hat{r} n_0 \tau$, \hat{r} is the coefficient of quadratic recombination

$$\Phi(h, N) = 1 + \frac{b_h}{\hat{b}_e} \left(\frac{h}{N+1} \right)^2,$$

$$\Psi(h, N) = 1 + \frac{b_h}{\hat{b}_e} h^2 + \frac{N}{N+1} \gamma^{-1}(E_\varphi, N) h^2.$$

Equations (1) and (2) were derived for the case when the electron mobility is much higher than the hole mobility ($b_h = 2 \times 10^6$ cgs esu for n -InSb and 7.5×10^7 for n -Bi $_{0.9}$ Sb $_{0.1}$, Ref. 9). for n -Bi $_{0.9}$ Sb $_{0.1}$, the indicated inequality holds in sufficiently strong electric fields⁹ $\gtrsim 5$ V/cm, appar-

ently on account of L - T intervalley transitions. In the case of the intrinsic plasma ($N \gg 1$) $\gamma = 1$, $\alpha = 0$, $G = 0$ the equations coincide with those obtained in Ref. 6.

We point out an important feature of the character of the magnetic-field penetration into the sample under conditions of ambipolar drift of the plasma to the axis. From the expression for the azimuthal electric field

$$E_\varphi = -\frac{c}{4\pi\sigma} \frac{\partial H}{\partial r} + \frac{v_{er}}{c} H,$$

obtained with the aid of the equations of motion and Maxwell's equation

$$\frac{\partial H}{\partial r} = \frac{4\pi}{c} e[(n+n_0)v_{e\varphi} - nv_{h\varphi}],$$

where $\sigma = e(n+n_0)b_e$ is the plasma conductivity and v_{er} is the velocity of the ambipolar electron drift $[(N+1)v_{er} = Nv_{hr}]$,

$$v_{i=e,h,\varphi} = \mp b_i E_\varphi \pm b_i v_{ir} H/c$$

are the azimuthal velocities of the electrons and holes, it follows directly that the equation for the magnetic field

$$\frac{\partial H}{\partial t} = -\frac{c}{r} \frac{\partial r E_\varphi}{\partial r}$$

contains besides the diffusion term

$$\sim \frac{1}{r} \frac{\partial}{\partial r} \left(D_H r \frac{\partial H}{\partial r} \right),$$

where $D_H = c^2/4\pi\sigma$, also a term corresponding to transport of the magnetic field by the ambipolar flux

$$\sim \frac{1}{r} \frac{\partial}{\partial r} (rv_{er} H).$$

As a result, the usual magnetic-field diffusion coefficient increases $\propto (1+h^2\gamma^{-1})$ in the region of high plasma density ($N > 1$). This nondiffusion mechanism of penetration of a magnetic field into a plasma was first investigated by numerical methods in Ref. 6.

We present expressions for the electric fields E_φ and E_r ,

induced by the alternating magnetic field:

$$E_\varphi(\rho) = -\frac{R_0}{\tau(b_h \hat{b}_e)^{1/2}} \frac{1}{\rho} \int_0^{\hat{\rho}} \frac{\partial h}{\partial T} \rho' d\rho', \quad (3)$$

$$E_r(\rho) = \frac{b_e H}{c} E_\varphi \Psi^{-1} \left(1 + \frac{h^2}{N+1} \frac{b_h}{\hat{b}_e} \right) - \frac{D_e}{b_e R_0} \frac{\partial N}{\partial \rho} \frac{1-h^2\gamma^{-1}}{(N+1)\Psi}.$$

The $g(E)$ dependence was chosen in the form¹³

$$g = g_0 \exp(-E_0/E_{\text{eff}}), \quad (4)$$

where

$$E_{\text{eff}} = (E_\varphi^2 + E_r^2)^{1/2} / (1 + \beta_H H),$$

and g_0 and E_0 are constants.

This choice of $g(E)$ is necessitated by the fact that in the case of transverse breakdown the decisive factor is the total electric field $E_t = (E_\varphi^2 + E_r^2)^{1/2}$, whose threshold value needed to obtain a plasma with $N > 1$ increases with the magnetic field.¹⁴ In the case of n -InSb we have $g_0 = 3.6 \cdot 10^9 \text{ sec}^{-1}$, $E_0 = 1700 \text{ V/cm}$, $\beta_H = 4 \times 10^{-4} \text{ Oe}^{-1}$ (Refs. 8 and 13); in n -Bi_{0.9}Sb_{0.1} we have $g_0 = 1.8 \cdot 10^{10} \text{ sec}^{-1}$, $E_0 = 34 \text{ V/cm}$, and $\beta_H = 5 \cdot 10^{-3} \text{ Oe}^{-1}$ (Ref. 9).

The initial system of equations was solved with a computer with initial and boundary conditions in the form $N(\rho, 0) = 0$, $h(\rho < 1, t = 0) = 0$, $\Gamma_\rho|_{\rho=1} = 0$ (the surface-recombination rate was assumed small), $h(\rho = 1, t) = h_0(t)$, where $h_0(t)$ is the magnetic field outside the sample, $\partial h / \partial \rho$ and $\partial N / \partial \rho|_{\rho=0} = 0$ as a result of the cylindrical symmetry.

The diffusion coefficients were determined from the Einstein relations under the assumption that the temperatures of the electrons and holes are equal to the energy of the optical photons ($\epsilon_{\text{opt}} \approx 0.025 \text{ eV}$ in InSb; 0.012 in Bi_{0.9}Sb_{0.1}). Since intense impact ionization is produced at $E \approx 200 \text{ V/cm}$ in n -InSb and at $E \approx 5 \text{ V/cm}$ in Bi_{0.9}Sb_{0.1} ($E \parallel C_3$) the sample size was chosen large enough, $R_0 = 0.5$ and 0.1 cm respectively, inasmuch as a given magnetic-field pulse the induced fields increase with increasing radius.

3. Let us discuss the results of the calculations in the

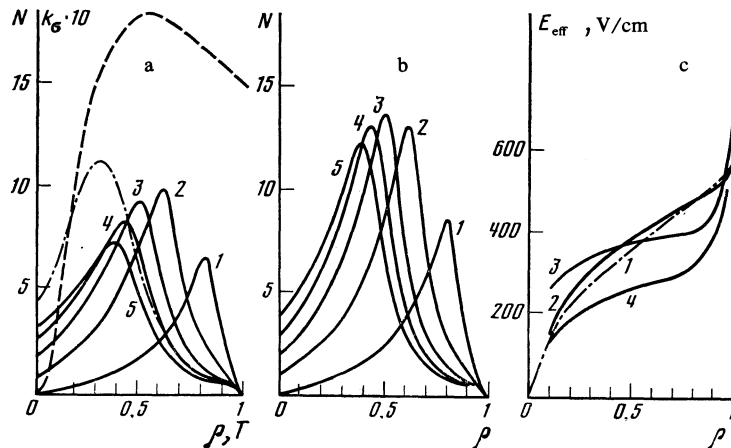


FIG. 1. θ pinch produced by a linear magnetic field pulse in n -InSb. a—Plasma density profiles at $n_0 = 2 \times 10^{14} \text{ cm}^{-3}$: 1–5) respectively at $T = 0.2, 0.4, 0.6, 0.8$, and 1.0 ; dashed curve—time dependence of sample conductivity; dash-dot curve—density profile at the end of the combined pulse, b—density profiles at $n_0 = 10^{14} \text{ cm}^{-3}$ (the values of T for curves 1–5 are the same as in case a), c—profiles of the effective electric field at $n_0 = 2 \times 10^{14} \text{ cm}^{-3}$: 1— $h_0 = 0.8$; 2—1; 3—2; 4—3.

case n -InSb. Figure 1 shows the profiles of the spatial density and of the effective electric field E_{eff} for a linear time dependence of the external magnetic field ($\tau = 10^{-7}$ sec, $h_{0 \text{ max}} = (b_h \hat{b}_e)^{1/2} H_{0 \text{ max}} / c = 10$, $H_{0 \text{ max}} \approx 20$ kOe) and for various donor densities. For the parameters indicated we have $\beta^2 \approx 3$ and 6, corresponding to a relatively weak skin effect, therefore the profile $E_\varphi(\rho)$ of the main part of the pulse ($h_0 > 3$) remains practically constant in time. As seen from the time scan of the plasma conductivity (Fig. 1a, dashed curve),

$$k_\sigma = \frac{2}{\hat{b}_e R_0^2} \int_0^{R_0} N b_e(E_\varphi) r dr,$$

and of the density of the profiles and of $E_{\text{eff}}(\rho)$ (Fig. 1c), particles are generated during the first half of the pulse, after which the predominant role is played by quadratic bulk recombination (the parameter r is assumed equal to $10^{-8} \text{ cm}^{-3} \cdot \text{sec}^{-1}$). The reason is that as the plasma presses towards the sample axis it enters into the region of a weaker field E_φ , and a role is also played by the decreases of E_{eff} on account of the magnetization. With increasing donor density the maximum values of $N(\rho, T)$ decrease, inasmuch as in this case the bulk recombination is more noticeable (the plasma density n is higher). The relatively small increase of k_σ is due to the low electron mobility, since the field $E_\varphi(\rho = 1) \approx 530 \text{ V/cm}$ is quite strong in the variant considered.

Figures 2 and 3 show analogous calculations as well as the magnetic-field profiles for a sinusoidal magnetic-field pulse at $h_{0 \text{ max}} = 3$ and $\tau = 1.2 \times 10^{-7}$ sec. These parameters correspond to the same mean values of the modulus of E_φ on the sample boundary as in the considered case of a linear pulse. The period of the pulse was divided into 40 parts and the numbers on the curves of Fig. 2 show the corresponding instants of time.

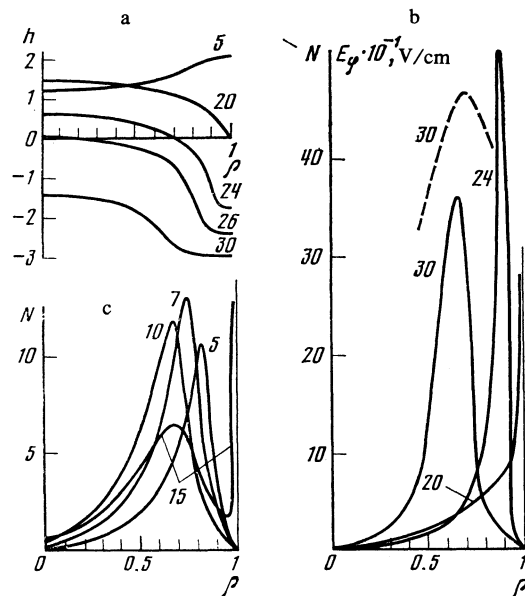


FIG. 2. Profiles of the magnetic field and of the plasma density for a harmonic magnetic-field pulse in n -InSb. The dashed curve in Fig. 2c is the profile of the azimuthal electric field at the end of the third quarter of the period.

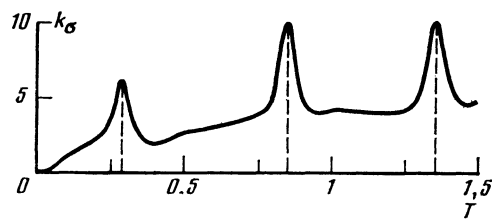


FIG. 3. Time scan of the sample conductivity for a harmonic magnetic-field pulse in n -InSb.

The first stage of the pinching of the plasma ($0 \leq T \leq 1/4$) take place with a weak skin effect of the magnetic field (Fig. 2a, curve 5), and at the end of the first quarter the value of the maximum of $N(\rho)$ decreases somewhat because of the decrease of E_φ ($E_\varphi \sim \cos 2\pi T$). At the same time the sample conductivity increases steeply (Fig. 3), owing to the increase of the electron mobility.

During the second quarter of the period the plasma is pressed towards the boundary of the sample (E_φ reverses sign). The preliminary ionization during the first quarter produces a barrier for the magnetic field (Fig. 2a, curve 20; Fig. 2b-15) and at the end of the second quarter (Fig. 2a, curve 20) the magnetic field is trapped. The subsequent pinching takes place under strong skin-effect conditions (Fig. 2a, curves 24, 26, 30), and in this case a neutral current layer is produced (the magnetic field reverses sign in this region and the particles move from the opposite direction). The appreciable growth of the plasma density at the end of the third quarter of the period and the increase of the conductivity (Fig. 3) are due to the increase of the E_φ field in the central region of the sample (Fig. 2c, dashed curve, as well as Fig. 2a, curves 20, 24, 26, and 30, from which the value of E_φ can be assessed). The maximum E_φ practically coincides with the maximum of $N(\rho, T)$. We note that formation of a neutral current layer during the third quarter of the period was observed in Ref. 4. The succeeding pinching phases during odd quarters of the period do not lead to a noticeable increase of the conductivity and density of the plasma (Fig.

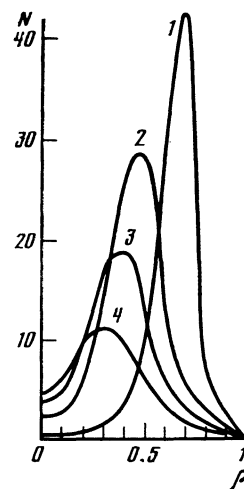


FIG. 4. Density profiles for combined magnetic-field pulse in n -InSb at $n_0 = 2 \times 10^{14} \text{ cm}^{-3}$ (stage of pinching by a linear pulse): 1 - $h_0 = 3$; 2 - 4.5; 3 - 6; 4 - 9.

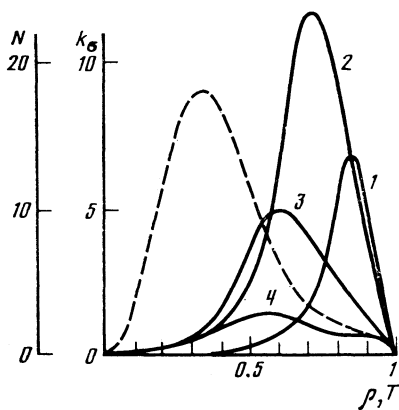


FIG. 5. θ pinch in $\text{Bi}_{0.9}\text{Sb}_{0.1}$ (linear pulse); Curves 1–4) density profiles at $T = 0.175, 0.35, 0.525,$ and $0.7,$ respectively; the dashed curve is the time dependence of the conductivity.

3), since an abrupt increase takes place in the quadratic bulk recombination that stabilizes the plasma accumulation ($N(\rho, T = \frac{3}{4}) \approx N(\rho, T = \frac{1}{4})$).

To obtain a higher plasma density at the center of the sample we can use a combined magnetic-field pulse, with the preionization produced by a sinusoidal pulse and the succeeding pinching by the linear pulse. Figure 4 shows a plot of $N(\rho, T)$ for this case: one period of a sinusoidal magnetic field is first applied to the sample. The parameters of these pulses are similar to those considered above. The plasma density towards the end of the pulse is considerably higher than in the case of a simple linear pulse (compare curves 5 with the dash-dot curve of Fig. 1a). At the same time, as seen from Fig. 4, the process of pinching of the plasma towards the axis is accompanied by an appreciable loss of electron-hole pairs to recombination.

4. We present below the calculations for the compound $\text{Bi}_{0.9}\text{Sb}_{0.1}$. This alloy is characterized by a relatively low anisotropy of the carrier mobility ($\approx 25\%$) and by a strong anisotropy of the impact-ionization coefficient.⁹ The largest values of b_e and g are realized when E is parallel to the trigonal axis ($E \parallel C_3$). The calculations were therefore made for the case when the pulsed magnetic field was directed along a binary or bisector axis ($H \parallel C_1$ or C_2), so that the transverse breakdown was realized at the maximum rate of impact ionization. The electron mobility was assumed to be isotropic and was chosen in the form

$$b_{e0} = \hat{b}_{e0} / [1 + (E_{\varphi}/E_0)^{1/2}],$$

where $E_0 = 10$ V/cm and $\hat{b}_{e0} = 1.5 \cdot 10^9$ cgs esu. This equa-

tion agrees with the measurement data.¹¹ In the case of a θ pinch ($H \parallel C_1$) the fields E_{φ} and E_r lie in the plane of the axes C_2 and C_3 . For g we chose its maximum value. Account was taken in the continuity equation of the linear and cubic recombinations, and the corresponding coefficients were assumed equal to⁹ $r_1 = 2 \cdot 10^8 \text{ sec}^{-1}$ and $r_3 = 10^{-23} \text{ cm}^6 \cdot \text{sec}^{-1}$. A linear magnetic-field pulse was considered ($\tau = 4 \cdot 10^{-8} \text{ sec}$, $h_{0 \text{ max}} = 7$, $H_{0 \text{ max}} \approx 1 \text{ kOe}$, $R_0 = 10^{-1} \text{ cm}$, $n_0 = 10^{14} \text{ cm}^{-3}$, and $D_n = 10^3 \text{ cm}^2 \cdot \text{sec}^{-1}$).

Figure 5 shows the density profiles for different instants of time. Just as in the case of n -InSb, the most effective is the initial stage of the pulse. The maximum increase of the density is reached at $T = 0.35$. The maximum increase of the sample conductivity is considerably higher than in the case of n -InSb (Fig. 1b), for in this variant the electric field is not strong enough to cause an appreciable decrease of the electron mobility.

In conclusion, we are deeply grateful to Yu. N. Yavlinkii for a helpful discussion.

¹L. A. Artsimovich, Controlled Thermonuclear Reactions, Gordon and Breach, 1964.

²W. Schneider, H. Groh, H. Bruhns, and K. Hubner, Sol. St. Comm. **9**, 1903 (1971).

³V. V. Vladimirov, L. V. Dubovoi, V. A. Smirnov, and V. F. Shanskii, Zh. Eksp. Teor. Fiz. **66**, 235 (1974) [Sov. Phys. JETP **39**, 111 (1974)].

⁴W. Schneider and K. Hubner, J. Phys. Chem. Solids **35**, 1297 (1974).

⁵Yu. N. Yavlinkii, Fiz. Tverd. Tela (Leningrad) **12**, 3385 (1970) [Sov. Phys. Solid State **12**, 2755 (1971)]; V. V. Vladimirov and Yu. N. Yavlinkii, Zh. Eksp. Teor. Fiz. **60**, 2344 (1971) [Sov. Phys. JETP **33**, 1257 (1971)].

⁶V. V. Vladimirov, V. N. Gorshkov, and Yu. N. Yavlinkii, Zh. Eksp. Teor. Fiz. **69**, 750 (1975) [Sov. Phys. JETP **42**, 383 (1975)]; H. Bruhns and K. Hubner, Appl. Phys. **6**, 215 (1975).

⁷M. Toda and M. Glicksman, Phys. Rev. **140A**, 1317 (1965).

⁸K. Gyubner and M. Markus, Proc. 9-th Internat. Conf. on Semiconductor Physics, Moscow, 1968, Vol. 2, p. 887.

⁹N. B. Brandt, E. V. Bogdanov, V. M. Manankov, and G. D. Yakovlev, Fiz. Tekh. Poluprovodn. **15**, 813 (1981) [Sov. Phys. Semicond. **15**, 465 (1981)]; E. V. Bogdanov, V. V. Vladimirov, and V. N. Gorshkov, Zh. Eksp. Teor. Fiz. **84**, 1468 (1983) [Sov. Phys. JETP **57**, 854 (1983)].

¹⁰A. Neukermans and G. S. Kino, Phys. Rev. **B7**, 2703 (1973).

¹¹N. B. Brandt, E. A. Svistov, E. A. Svistova, and G. D. Yakovlev, Zh. Eksp. Teor. Fiz. **61**, 1078 (1971) [Sov. Phys. JETP **34**, 575 (1972)].

¹²E. Conwell and V. F. Weiskopf, Phys. Rev. **77**, 388 (1950).

¹³V. V. Vladimirov, V. N. Gorshkov, A. G. Kollyukh, and V. K. Malyutenko, Zh. Eksp. Teor. Fiz. **82**, 2001 (1982) [Sov. Phys. JETP **55**, 1150 (1982)].

¹⁴H. Schmidt and D. Nelson, Phys. Rev. **184**, 760 (1969); A. A. Andronov, V. A. Valov, V. A. Kozlov, and L. S. Mazov, Preprint No. 2, Inst. Appl. Phys., USSR Acad. Sci., Gorky, 1981.

Translated by J. G. Adashko